

EFFICIENT REMOVAL OF METHYLENE BLUE DYE FROM AQUEOUS SOLUTION USING A NEW BIOSORBENT DERIVED FROM *ENSETE VENTRICOSUM* (ENSET)

Belete Tewabe Gebeyehu^{1*}, Daniel Manaye Kabtamu^{1,2} and Temesgen Alehegne Tasew¹

¹Department of Chemistry, Debre Berhan University, Debre Berhan, Ethiopia

²Department of Materials Science and Engineering, National Taiwan University of Science and Technology, Taipei, Taiwan

(Received August 25, 2023; Revised October 23, 2023; Accepted October 26, 2023)

ABSTRACT. In this study, kocho was prepared from pseudostem and corn of *Ensete ventricosum* (*enset*). The behaviors of kocho were examined by using FESEM, TGA, XRD and FTIR spectroscopy. The biosorption potential of kocho, a possible low-cost new biosorbent for the efficient removal of MB dye from wastewater was investigated. Biosorption experiments were carried out in batch mode to study the effects of biosorbent dosages (0.025-0.2 g), pH (2–10), initial concentrations of MB (10 to 100 mg/L) and contact time (10 to 120 min). The highest removal efficiency of methylene blue dye (94.2%) was recorded at optimum experimental conditions. Following the removal study, it was determined that the pseudo-second order kinetics ($R^2 = 0.997$) and Langmuir isothermal ($R^2 = 0.996$) models may well describe the MB dye biosorption process. Furthermore, this newly developed biosorbent was fairly recyclable up to five cycles without significant loss of re-adsorption efficiency (around 9.6% loss) between 1st and 5th cycle. Thus, the findings of this study revealed that a new kocho biosorbent derived from *Ensete ventricosum* can be used as a promising low-cost, environmentally friendly and efficient biosorbent for the rapid removal of MB from aqueous solutions.

KEY WORDS: Kocho, *Ensete ventricosum*, Biosorption, Methylene blue, Kinetics, Isothermal

INTRODUCTION

Clean and safe water is vital to human health and happiness, ecosystems, and a thriving economy. However, the presence of pollutants [1, 2] such as pesticides, heavy metals, fertilizers, dyes, etc. in water systems can lead to degraded water quality, resulting in detrimental effects on organisms and human health. Among these pollutants, dyestuffs emitted by the industries are a major environmental challenge facing the world.

Dyes are largely used in the manufacturing of various industrial products such as rubber, plastics, cosmetics, textiles, food, leather, pulp and paper [3, 4]. Recently, the release of toxic dyes into water streams by industries has received increasing attention due to the adverse effects of these wastes [5]. By their nature, exposure time and concentration, dyes may cause serious health effects such as skin irritation, respiratory disorders, mental disturbances, vomiting, and in many cases they may be carcinogenic and mutagenic [6, 7]. For example, methylene blue ($C_{16}H_{18}N_3SCl$), a cationic dye used in a variety of industries to dye cotton, wool and silk has several harmful effects on the human body, including increased heart rate, nausea, shock, respiration distress, quadriplegia and necrosis [8]. Therefore, there is a need for efficient and economical methods to remove dyes from wastewater to protect local populations and maintain environmental health.

Several conventional treatment methods [2, 9] were used to remove contaminants from wastewater, including flocculation/coagulation, adsorption, precipitation, membrane separation electrochemical processes and solvent extraction. However, most of these techniques lack the advantages of being fast, selective, efficient, economical and/or environmentally friendly. Among these techniques, adsorption is considered to be efficient and cost effective method for the

*Corresponding author. E-mail: beletetewabe@gmail.com, beletetewabe@dbu.edu.et

This work is licensed under the Creative Commons Attribution 4.0 International License

treatment of dye loaded wastewater. The removal of dyes from wastewater is thus made possible by the adsorption of different contaminants on efficient, economical and environment-friendly bio-wastes [4, 9-11]. Many researchers opt to use biosorbents for the removal of dyes instead of chemical adsorbents/chemically modified adsorbents as they provide promising results with a minimum disposal problem, since the biosorbents could be degraded easily by microorganism.

In order to remediate dye-contaminated water, low cost biosorbents derived from agricultural, residential and industrial wastes have been used as effective substitutes [3, 9, 12-14]. Biosorbents have been shown to have significant dye-binding capabilities due to the presence of proteins, polysaccharides, or lipids with functional groups like carboxyl, hydroxyl, amino, and sulfate on the surfaces of their cell walls.

Ensete ventricosum (enset) is a monocarpic tall perennial herbaceous plant which belongs in the order Scitamineae, family Musaceae and genus *Ensete* [15]. Enset is frequently referred to as "False Banana" since it looks similar to a banana tree but doesn't yield bananas. It has amazing weather resistance, making it one of the significant native crops that may be used for many different purposes by Ethiopians; including human nourishment, industrial fiber, animal feed, rob material, for building fences and homes, making chairs and beds, local packaging, and as a substitute for tableware or umbrellas [16, 17]. Enset plants typically have leaf lamina, leaf midribs, pseudostem and corm and root as basic parts.

The pseudostem and corm are the most important enset plant components in terms of biomass. Kocho traditional culinary item in the central and southern regions of Ethiopia [18], is created when these two ingredients are combined and fermented. Kocho is fermented composite product made from the pseudo stem and corm of *Ensete ventricosum*. However, in most parts of Ethiopia and the rest of the world, pseudostem and corm of enset plant are considered as waste products.

Several low cost biosorbents such as tea waste, fava bean peel [9], rice husk [19], banana fibre [20], coconut fibre [20], sawdust [20], barley bran [21], enset midrib leaf [21], eucalyptus sheathina bark [22], solanum tuberosum [23], pisum sativum peels [23] and rice straw [24] have been reported in literature for the removal of dyes. However, to the best of our knowledge the use of kocho for the remediation of methylene blue (cationic model dye) present in wastewater has not been reported yet. Therefore, this study investigated the suitability of kocho as low cost and ecofriendly biosorbent for the removal of methylene blue (MB) from wastewater. The effects of several factors influencing the adsorption of dyes such as adsorbent dosage, initial dye concentration, pH and contact time were studied. Moreover, many characteristics related to adsorption kinetics and isotherms were determined. Adsorption-desorption tests were also used to look at the biosorbent's regeneration abilities. Thus, we believe this study provides a new route towards the development of a new biosorbent for efficient removal of dyes with a wide range of water treatment applications.

EXPERIMENTAL

Materials and reagents

Methylene blue (MB, chemical formula – $C_{16}H_{18}ClN_3S$, molecular weight: $319.85 \text{ g mol}^{-1}$, 98% dye content) was obtained from Aladdin Co., Ltd., China. The stock solutions (100 mg L^{-1}) of MB were prepared by dissolving accurately weighed amount of the dye in distilled water. All the chemicals used throughout this study were of analytical-grade. All working solutions of required concentrations were obtained by diluting the stock solution with distilled water. The pH value of water was adjusted by 0.1 M HCl and/or 0.1 M NaOH.

Preparation of kocho powder sample

The kocho powder was prepared from pseudostem and corm of enset by fermentation. Briefly, matured enset plants were identified by locally established maturity signs, such as size of the

central shoot, appearance of inflorescence and exposure of the corm. The pseudostem and corm from matured enset plants were washed, cut, diced and crushed traditionally. The oozing liquid containing starch was collected from the pseudostem part and mixed with corm one. For the production of kocho powder, pseudo-stem, corm and starter amicho (previously fermented decorticated enset pseudostem) were mixed together for about one month. The fermentation process was carried out in a ground pit at a temperature about 25-30 °C, anaerobic fermentation. Finally, the local fermentation product known as kocho was carefully rinsed with tap water before being washed with distilled water. It spent 48 hours at 70 °C in the oven. The dried kocho was then ground to a fine powder kocho using a steady arm grinder and the fine powder was chosen for the biosorption experiments.

Instruments

FE-SEM (JEOL, Tokyo, Japan), thermo gravimetric analyzer (TGA instruments, UDA), diffractometer (Rigaku, RINT 2000), FTIR spectroscopy (Bruker, Germany) and UV-Vis spectrophotometer (V-650, JASCO, Japan) were used to analysis different parameters.

Characterizations

Analyses of the morphology of pristine kocho were investigated using field emission scanning electron microscope (FESEM). The sample was first coated with a thin layer of platinum in a vacuum chamber for 60 seconds before imaging. For FESEM observation, the samples were stuck with the help of carbon tape onto a stub of 1 cm diameter. The FESEM image was taken in secondary electron mode with a beam of energy 15.0 kV.

For the thermal gravimetric analysis (TGA), kocho samples (~3 mg) were loaded to a platinum sample pan and heated in nitrogen from 25 to 105 °C at 20 °C/min. After incubating at 105 °C for 10 min, it was heated further from 105 to 800 °C at a heating rate of 20 °C/min.

The crystallographic information for the synthesized kocho was gathered from powder X-ray diffraction studies performed with Cu-K α ($\lambda = 0.154$ nm) radiation at a voltage of 40 kV and tube current of 30 mA. The scanning range was from 10–80 and the scan rate was 2 min⁻¹.

The FTIR spectra of the pristine kocho (before biosorption of MB) and the MB-loaded samples (dose of biosorbent 0.1 g, 50 mg/L MB for 50 min) were obtained using a FTIR spectrometer accumulating 64 scans at a spectral resolution of 1 cm⁻¹ in the range of 4000–400 cm⁻¹. Each sample was finely ground and then mixed with KBr at a ratio of 1/50 (mg/mg) and pressed to prepare the pellet.

Batch biosorption experiments

Batch experiments were conducted to get equilibrium data and validate the best parameters for the biosorption treatment process. Different factors affecting the biosorption of MB dye including the biosorbent dosage (0.01-0.2 g), initial concentrations MB (10-100 mg/L), the pH solution (2-10) and contact time (10-120 min) were measured at a constant agitation speed of 200 rpm and a temperature of 278 K in a batch mode. Dosage-dependent removal efficiency experiments were done using different kocho dosages (0.01, 0.025, 0.05, 0.1, 0.15 and 0.2 g) at optimum experimental conditions (20 mL of 50 mg/L MB, pH (8) and incubation time 50 min).

To study the effect of pH on removal efficiency, 20 mL MB dye solutions (50 mg/L) were incubated for 50 min with 0.1 g kocho under various pH values (2, 3, 4, 5, 6, 7, 8, 9 and 10). Furthermore, to investigate the effect of MB dye concentrations, 20 mL dye solutions with various concentrations (10, 25, 50, 75 and 100 mg/L) were incubated for 50 minutes after mixing with 0.1 g of kocho powder. Finally the effects of different contact time (10, 20, 30, 40, 50, 60, 90 and 120 min) were analyzed by mixing 20 mL MB dye solutions (50 mg/L) and dose of kocho (0.1 g) at pH 8. For each experiment, after filtering the agitated adsorbate solution over a 0.22 μ m

microfiltration membrane, the remaining MB dye concentration in the filtrate was measured using a UV-Vis spectrophotometer. The following equations were applied to compute the amount of dye adsorbed at preset time t (q_t , mg/g), equilibrium adsorption amount (q_e , mg/g) and removal efficiency (R , %) of biosorbent (kocho).

$$q_e = (C_o - C_e) \times \frac{V}{m} \quad (1)$$

$$q_t = (C_o - C_t) \times \frac{V}{m} \quad (2)$$

$$\% \text{ Removal} = \frac{(C_o - C_t)}{C_o} \times 100 \quad (3)$$

where C_o (mg/L) is the initial concentration of the MB dye, C_t (mg/L) is the concentration of MB dye at any time, C_e (mg/L) is the liquid-phase dye concentration at equilibrium, V (L) is the volume solution and m (g) is the mass of the biosorbent.

Determination of point of zero charge (PZC) of the kocho

The pH of the point of zero charge (pH_{PZC}) of kocho was determined by salt addition method [25]. The pH was adjusted with 0.1 M HNO_3 and 0.1 M NaOH using a digital pH meter as needed, to obtain the appropriate pH range of 2, 3, 4, 5, 6, 7, 8, 9, 10 and 11. After mixing with 0.1 g of the kocho sample, the solutions were shaken for 24 h using an agitator at 200 rpm. The pH values of the supernatant in each tube were measured and denoted as pH_f . The pH_{PZC} is obtained from the plot of ΔpH versus pH_i , where the point of intersection of the graph is equal to zero. Each set of experiment was performed in triplicate and the mean value was recorded.

Desorption studies

Solvents such as alcohols, alkalis, and acids were used as desorbents for removing the sorbates from the biosorbents [26, 27]. Therefore, to perform regeneration of kocho, the adsorbed MB dye on the surface of kocho was initially treated with HCl (0.1 M) followed by drying the free biosorbent in an oven at 70 °C. After each regeneration, a batch biosorption experiment was conducted to estimate the kocho regeneration ability using dose (0.1 g), MB concentration (C_o = 50 mg/L), contact time (50 min), pH(8) and agitation speed (200 rpm) at 278 K for a total of five cycles of adsorption-desorption processes. The MB dye load kocho was taken out from the dye solution and washed with distilled water for several times, and then dried. The dye loaded kocho was added into 20 mL 0.1 M HCl and stirred for 6 h. The process was repeated for five successive cycles. The percentage of desorption is calculated using Eq. (4).

$$\% \text{ Desorption} = \frac{\text{Concentration of desorbed dye (mg/L)}}{\text{Concentration of adsorbed dye } \left(\frac{\text{mg}}{\text{L}}\right)} \times 100 \quad (4)$$

RESULTS AND DISCUSSION

The biosorbent (kocho) was used to remove methylene blue from an aqueous solution. The experimental results of this newly developed biosorbent and the discussion of the outcomes from characterization, optimization, kinetics and isotherms studies were presented in this section.

Characterizations

Figure 1 shows field emission scanning electron microscopy (FESEM) images of the kocho powder sample at different magnifications. It is obvious from FESEM images (Figure 1a and b) that the surface of kocho is mostly dispersed by highly heterogeneous porous structures and cave

type apertures of various sizes. The kocho may therefore be a suitable biosorbent and has sufficient morphology for MB dye biosorption in wastewater treatment.

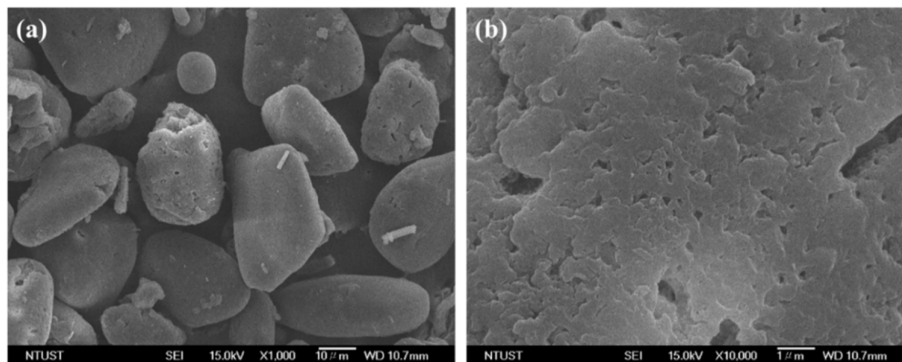


Figure 1. FESEM images of the kocho morphology at different magnifications of: (a) x 1, 000 and (b) x 10, 000.

Thermogravimetric analysis (TGA)

TGA analysis was performed to determine mass losses and thermal property of the kocho. The thermogravimetric profile of the kocho as a function of temperature is shown in Figure 2a. The decomposition of the kocho occurs in multistep processes. The first step (weight loss (7%)) occurred around 120 °C due to the elimination of water molecules from the surface of the kocho biomass. The second step registered consistency, the thermal stability of kocho and then decrease of weight started at 270 °C and persisted until 340 °C, which may be due to the decomposition of carbon-based functional groups (cellulose) [28]. The deterioration temperature was then started at 370 °C and showed quick weight loss (80%) up to 540 °C. After that, the final decomposition may be seen, where a maximum component in the kocho was decomposed. The overall weight loss (98%) corresponds to the loss of carbon and oxygen due to the decomposition of kocho's lignocellulosic components. This could be explained by the presence of lignin, which protects the cellulose chains in the cell wall.

X-ray powder diffraction (XRD)

X-ray diffraction (XRD) instrument was used to characterize the crystallite nature of kocho powder. Figure 2b shows the typical XRD spectrum of the degree of crystallinity and amorphosity of kocho. The XRD pattern of the kocho shows peaks at around $2\theta = 14.86, 17.03, 22.11, 23.99^\circ$, and 26° , corresponding to the signals of carbon materials (JCPDS no. 01-075-2078), as shown in Figure 2b.

The crystalline phase of kocho cellulose correlates to the highest diffraction intensity, which was discovered at $2\theta = 17.03$. The amorphous phase of kocho lignocellulose is represented by the diffraction intensity obtained at $2\theta = 23.99^\circ$, which is the least intensity. In addition, few diffused peaks at higher 2θ values indicate the decrease in crystallinity of the cellulose and correspond to amorphous phase of lignin and hemicellulose. In agreement of this research, other researchers have also noted the broad peaks at about 16° and 22° in a variety of woods, including rubber wood sawdust, pinewood, and *Pinus elliotii* plantation wood [10].

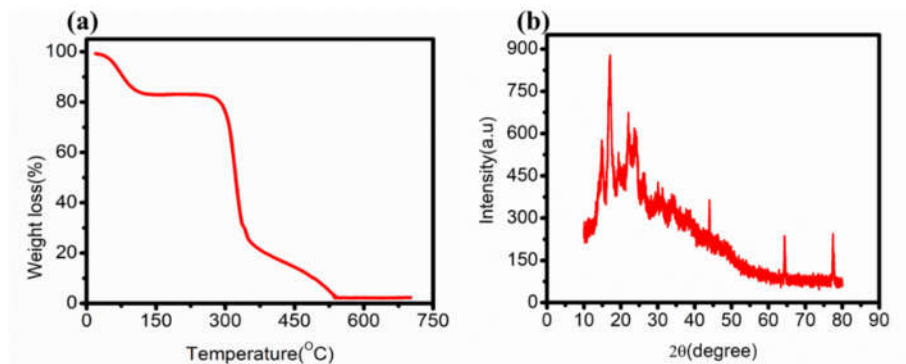


Figure 2. (a) TGA of kocho and (b) XRD pattern of kocho.

Fourier transform infrared spectroscopy (FTIR) analysis

The FTIR spectra of kocho were analyzed before and after MB biosorption (Figure 3) to detect any differences due to the interaction between the functional groups on the biomass and MB dye during biosorption process [29]. As can be seen in Figure 3, the pristine kocho main peaks appeared at 3674, 3272, 2901, 2888, 1635, 1452, 1394, 1250, 1150, 1075, 1066, 1048, 1015, 892 and 571 cm^{-1} . The peak at 3676 cm^{-1} is ascribed to the free -OH stretching vibrations. The broad peak at 3269 cm^{-1} is attributed to -OH stretching vibrations due to inter and intramolecular hydrogen bonding of macromolecular associations, such as alcohols, phenols and carboxylic acids, cellulose and lignin, thus showing the presence of hydroxyl groups “free” on the surface of the adsorbent [30]. The peaks at 2901 and 2888 cm^{-1} can also assign to the C-H stretching of lignocellulosic components. The characteristic peak at 1635 cm^{-1} shows the presence of the ester (C=O) linkage of the carboxylic group of lignin and hemicelluloses [31]. Other prominent peaks are C-O-C stretching vibrations (1075 cm^{-1}), C-O stretching (at 1252 cm^{-1}), C=O (1066 cm^{-1}), C-O-C deformation (at 1048 cm^{-1}), and glycosidic linkage at 892 cm^{-1} . Therefore, the peaks in pristine kocho show the presence of cellulose, hemicellulose and lignin in the selected biosorbent [32].

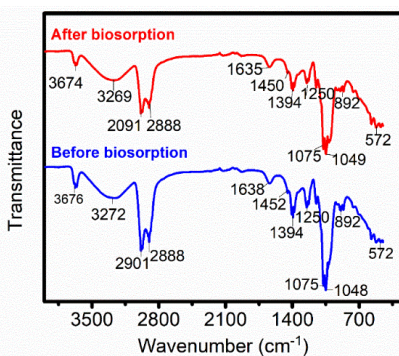


Figure 3. FTIR spectra of kocho before and after biosorption of MB dye.

As shown in Figure 3, some distinct changes are observed between the spectra before and after methylene blue biosorption on biomass. The increase in intensity and shift in peak positions in kocho following MB biosorption demonstrates the involvement of different functional groups during the biosorption. Figure 3 clearly illustrates the shift in peak locations from 3676 to 3675, 3272 to 3269, 1635 to 1638 and 1450 to 1452 cm^{-1} following the biosorption process. The change in some of FTIR spectra confirmed the inclusion of methylene blue dye with functional groups present in the biomass. These may result from an interaction between the positive centers of the MB dye and the negative centers of the kocho biosorbent, which involves significant attractive forces. Based on previous studies, the various functional groups from cellulose, hemi-cellulose and lignin contained in biomass have a beneficial effect by generating active binding sites for dye adsorption through different mechanisms [32, 33].

Effect of various parameters on dye biosorption

The dosage, initial concentration of the MB, pH and contact time are some of the crucial variables that affect how well dyes adhere to biosorbent surfaces. In this study, the effect of one parameter on the MB dye biosorption process could be monitored when the other parameters are kept constant. Following the description of the pristine and loaded kocho, a thorough investigation of how these variables impact the biosorption of cationic contaminant (MB) dye is briefly presented in the following sections.

The effect of dosage

The biosorbent should be able to adsorb a sizable amount of adsorbate at low doses in an effective removal process with minimal operating costs. In this study, the effect of dosage of biosorbent on the removal efficiency of MB dye was investigated by varying the amounts of kocho (0.01, 0.025, 0.05, 0.1, 0.15 and 0.2 g). For this purpose, specific amounts of kocho were added in 20 mL MB dye solutions at room temperature using an optimized pH (8), initial MB concentration (50 mg/L), contact time (50 min) and 200 rpm agitation. As shown in Figure 4a, when the amount of biosorbent dosage was elevated from 0.01 g to 0.1 g, the removal of efficiency of MB increased dramatically from 57.18% to 94.2% and after that the increase was only marginal. Although a slight increase in the percentage biosorption was observed at adsorbent amounts higher than 0.1 g, the subsequent biosorption studies were carried out using 0.1 g of biosorbent for the sake of simplicity and process efficiency. Biosorption typically increases as adsorbent amounts rise, which is caused by an increase in surface area [4, 11, 34]. However, there comes a point where adding more biosorbent does not further increase biosorption; instead, it stays virtually constant.

Effect of initial MB dye concentration

The removal of methylene blue dye from aqueous solution was evaluated by varying MB initial concentration in the range of 25-100 mg/L at pre-optimized dose (0.1 g), pH (8) and contact time (50 min) at agitation of speed 200 rpm. As shown in Figure 4b, the percentage of removal for kocho biosorbent reduced from 98% to 64% when the initial MB concentration increased from 10 mg/L to 100 mg/L, respectively. About 97%, 94.2% and 80% percent elimination was accomplished with dye doses of 25, 50 and 75 mg/L, respectively (Figure 4b). This trend can be attributed to the saturation of the active sites for biosorption on the biosorbent surface at higher concentrations of dyes. Moreover, this is explained by the fact that fewer dye molecules were accessible and occupied the open adsorbent sites at lower starting MB concentrations [34, 35]. This is a common phenomenon in the biosorption process and revealed in results of previous studies on removal of MB by pine cone [36], oak sawdust [37] and activated carbon from rice husk [38].

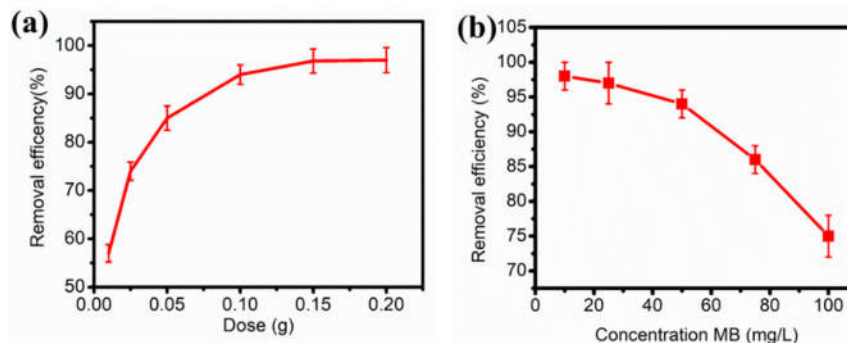


Figure 4. (a) Effect of biosorbent dosage on removal efficiency; ($C_0 = 50$ mg/L, contact time = 50 min and pH = 8) and (b) effect of initial MB concentration on removal efficiency (dose = 0.1 g, contact time = 50 min and pH = 8).

Effect of initial pH

Depending on the chemical structure of the dye and biosorbent, pH has a noticeable effect in affecting the biosorption capacity of the adsorbent. It influences the adsorbent's surface charge as well as the functional groups' degree of protonation [34, 39]. Here in, using an initial MB dye concentration of 50 mg/L and 0.1 g biosorbent, the influence of pH on MB adsorption of the kocho at 50 min was examined in the pH range of 2-10. The pH of dye solutions was adjusted by using 0.1 M aqueous sodium hydroxide and 0.1 M aqueous hydrochloric acid solutions.

In the pH range of 2 to 8, as depicted in Figure 5a, the clearance rate increased quickly from 29.2% to 94.2%. However, the highest biosorption was at pH 10 (95.4%, 9.54 mg/g), whereas the lowest removal was at pH 2 (29.2%, 2.9 mg/g). And also for pH 3 (34.3%, 3.4 mg/g) to pH 8 (94.2%, 9.4 mg/g), the removal percentage and biosorption capacity of MB dye on kocho increased with increased in solution pH. A slightly lower percentage removal observed at pH 2 compared to pH 3 can be attributed to a higher extent of protonation of carboxylic functional group resulting in the reduction in net negative change on the dye molecules that led to a reduced electrostatic interaction between kocho MB dye. Increase in the removal efficiency at pH 6 (74.3%, 7.4 mg/g) and above can be related to the decrease in the extent of protonation of functional groups of the biosorbent.

The surface of the kocho gained a negative charge when the pH of the dye solution rises, which led to an increase in the MB's biosorption as a result of an increase in the electrostatic attraction between the negatively charged adsorbent and the positively charged dye. Due to competition between the increased H^+ and the cationic dye for the kocho group biosorption sites, the biosorption was unfavorable in an acidic environment. It is evident that the amount of MB adsorbed was significantly influenced by the pH of the solution. As a result, these findings revealed that alkaline conditions were preferred over acidic ones for removal efficiency. This implies that alkalinity improves the electropositive biosorption of materials where acidity decreases the biosorption of positively charged dye due to electrostatic repulsion [4, 40]. On the other hand, the lower uptake rate of cationic dyes at acidic pH may be attributed to the excess presence of (H^+) ions competing with the dye cation groups for biosorption sites. Similar findings on MB adsorption onto banana peel powder, papaya seeds, bamboo and banana stem debris, garlic peel, grass waste, yellow passion fruit peel and citrus limetta peel, were also reported [4, 11, 41]. The point of zero charge (pHpzc), an attribute of adsorbents, can better explain the significant impact of pH on adsorption. The adsorbent surface is neutral at $pH = pH_{pzc}$ (zero-point charge),

negatively charged at $\text{pH} > \text{pHpzc}$, and positively charged at $\text{pH} < \text{pHpzc}$. In this study, the PZC was obtained from the plot of ΔpH ($= \text{pH}_f - \text{pH}_i$) against pH_i , where the point of intersection of the graph is equal to zero. As shown in Figure 5b, the pHpzc of the kocho biosorbent was determined to be 5.69. This demonstrates that the surface has a positive charge due to protonation at $\text{pH} < 5.69$ whereas the adsorbent surface gets a negative charge due to deprotonating in the excess of hydroxyl ions at $\text{pH} > 5.69$. As a result, the kocho's removal of MB cationic dye was most effective at $\text{pH} > \text{pHpzc}$ where the functional groups get protonated and less MB dye are adsorbed by the biosorbent. The approximately close values were reported for other biosorbents: 5.6 for raspberry (*Rubus idaeus*) leaves powder [42], 5.77 for *Syringa vulgaris* leaves powder [43], 6.3 for papaya leaf powder and *Typha angustifolia* leaves powder [44].

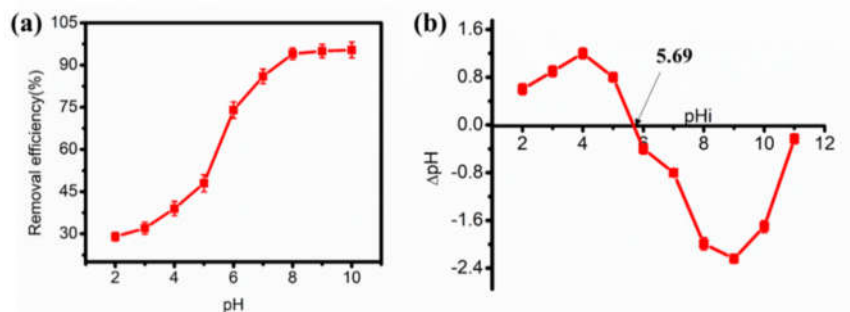


Figure 5. (a) Effect of pH on removal efficiency; ($C_0 = 50 \text{ mg/L}$, dose = 0.1 g and contact time = 50 min) and (b) determination of zero point of charge (pHpzc) of kocho.

Effect of contact time

The effect of contact time on the biosorption of MB was examined to determine the optimum time required for the maximum uptake of dye for various time intervals ranging from 10 to 120 min (Figure 6a). According to Figure 6a, the MB dye quickly adsorbed to the surface of kocho in the first 40 minutes and then the rate of adsorption declines until equilibrium is reached around 50 minutes. A further increase in the contact time did not result in any appreciable increase in the removal percentage and for the sake of process simplicity and efficiency; all the subsequent adsorption studies were performed using contact times of 50 min.

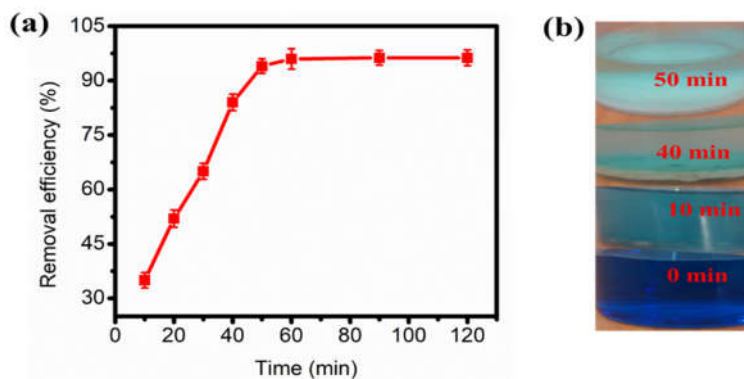


Figure 6. (a) Effect of contact time on removal efficiency; ($C_0 = 50 \text{ mg/L}$, dose = 0.1 g and $\text{pH} = 8$) and (b) discoloration of MB dye at different incubation times with kocho.

Additionally, the discolorations of the MB solution under different adsorption times are shown in Figure 6b. When the kocho was used as the biosorbent, the color of the MB solution varied from dark blue to light blue. It finally became nearly transparent with the increasing biosorption time, which suggests that most of the MB molecules in the solution were adsorbed by the kocho. The presence of a large number of vacancies on the adsorbent surface that reached saturation at equilibrium is believed to be responsible for the sharp increase in adsorption capacity at the initial contact time. Due to a paucity of active sites for dye biosorption once equilibrium was established, it remains nearly constant.

Adsorption kinetics and isotherm model

Dye adsorption kinetics

In the adsorption mechanism, kinetic prediction of the adsorption capacity and adsorption time is crucial. The kinetic adsorption studies were conducted with an initial MB dye concentration of 50 mg/L, biosorbent dose of 0.1 g, pH (8) and contact time of 120 min at the agitation speed of 200 rpm. To assess the adsorption kinetics process, the pseudo-first-order [45] and pseudo-second-order [46] kinetic models were taken into consideration. These kinetic models are given by Eq. (5) and (6):

Pseudo-first-order:

$$\ln(q_e - q_t) = \ln q_e - k_1 t \quad (5)$$

Pseudo-second-order:

$$\frac{t}{q_t} = \frac{1}{k_2 q_e^2} + \frac{t}{q_e} \quad (6)$$

where, q_e and q_t (mg/g) are the sorption capacities at equilibrium and at time t , respectively.

The adsorption kinetic models can be used to predict the equilibrium adsorption capacity and clarify the adsorption mechanism of MB onto the surface of the kocho. The kinetic models of pseudo-first-order and pseudo-second-order were built in accordance with the results of adsorption experiments, as shown in Figure 7a, b and Table 1. The values of q_e , R^2 , k_1 and k_2 in Table 1 were obtained from the linear plots.

Table 1. Kinetic parameters for the biosorption of MB dye by kocho.

Kinetic mode	Kinetic parameter	Values
Pseudo first order	$k_1 \times 10^{-2}$ (min ⁻¹)	10.7
	q_e , cal (mg/g)	7.26
	q_e , exp (mg/g)	9.63
	R^2	0.9454
Pseudo second order	$K_2 \times 10^{-2}$ (g/mg min)	6.36
	q_e , cal (mg/g)	11.72
	q_e , exp (mg/g)	9.63
	R^2	0.9743

The experimental value of q_e , 9.63 mg/g, did not agree well with the calculated one q_e , cal (7.21 mg/g) as obtained from the linear plots (Figure 7a) and the value of the correlation coefficient ($R^2 = 0.9454$) were relatively low (Table 1). This indicates that the biosorption process does not comply with the pseudo-first order rate model. The pseudo-second-order model showed a better fit to describe the biosorption of MB onto kocho with the calculated value q_e , cal (11.72 mg/g) closer to the experimental value q_e , exp value (9.63 mg/g) and a higher correlation

coefficient ($R^2 = 0.9743$) than the first-order kinetics model (Table 1). So it can be said that the pseudo-second-order kinetic model was followed during the biosorption of MB dye on the imaginary kocho, confirming that the biosorption should involve a chemical interaction between active sites of kocho and ionic groups present in the dye molecules. Similar type of conclusion was documented from biosorption study of methylene blue dye using rice (*Oryza sativa* L.) straw [47].

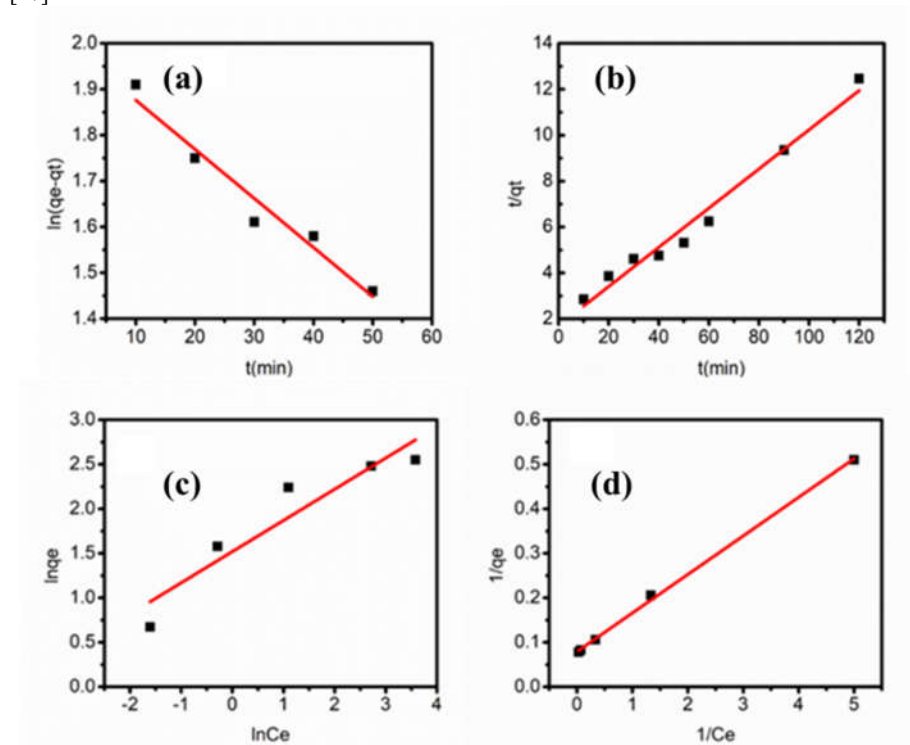


Figure 7. (a) Pseudo-first-order kinetics; (b) pseudo-second-order kinetics; (c) Freundlich adsorption isotherm and (d) Langmuir adsorption isotherm.

Adsorption isotherm

To shed light on how the adsorption achieved equilibrium and to pinpoint the interaction between the adsorbent and the adsorbate, Freundlich and Langmuir isotherms were used. The two models were evaluated to fit the isotherm data, and their linear plots are displayed in Figure 7(c), (d) and the related parameters were calculated from the two isotherms models (Table 2).

The Freundlich isotherm model was used to depict the adsorption on a heterogeneous surface. The adsorption on a surface with a heterogeneous energy distribution is represented using the Freundlich isotherm model [48]. The linear form of this model is written as (Eq. 7):

$$\ln q_e = \frac{1}{n} \ln C_e + \ln k_F \quad (7)$$

where q_e and C_e are the adsorbed MB amount (mg g^{-1}) at equilibrium and equilibrium concentration (mg L^{-1}), respectively. k_F ($\text{mg/g}/(\text{L/mg})^{1/n}$) is the Freundlich coefficient, which reflects the adsorption capacity and n is the Freundlich coefficient, which reflects the degree of

heterogeneity. For the favorable adsorption process, the value of n should be $1 < n < 10$. The plot of $\ln q_e$ versus $\ln C_e$ (Figure 7c) yields the slope ($1/n$) and intercepts ($\ln K_F$). From the slope and intercept values, n (2.87) and K_F ($4.57 \text{ (mg/g) (L/mg)}^{1/n}$) are determined, respectively (Table 2). Furthermore $1 < n$ (2.87) confirms the favorable nature of the adsorption process. The regression coefficient R^2 of the plot for Eq.7 is (0.855).

Table 2. Parameters for the Langmuir and Freundlich Isotherm equations.

Isotherm model	Isotherm constants	Values
Freundlich	N	2.85
	$K_F \text{ (mg/g)(L/mg)}^{1/n}$	4.57
	R^2	0.94426
Langmuir	$Q_m \text{ (mg/g)}$	11.54
	$K_L \text{ (L/mg)}$	1.0914
	R^2	0.99845

The Langmuir isotherm model, which may be written as (Eq. 8) relies on the assumption that the monolayer formation of the adsorbate molecules/ions over the surface of the adsorbent molecule through mainly chemical interactions between the adsorbate and adsorbent.

$$\frac{1}{q_e} = \frac{1}{q_m K_L C_e} + \frac{1}{q_m} \quad (8)$$

where q_e represents adsorption capacity at equilibrium, C_e represents equilibrium concentration, q_m denotes maximum adsorption capacity and K_L denotes the Langmuir constant (L mg^{-1}), which is a measure of the free energy of adsorption and is associated to the affinity of the binding site. The plot of $1/q_e$ versus $1/C_e$ is shown in Figure 7d, and the slope and intercept obtained from the plot are used to determine K_L (1.09 L mg^{-1}) and q_m (11.54 mg g^{-1}), respectively, (listed in Table 2). Additionally, the Langmuir adsorption constant, K_L , is related to the separation factor, R_L , as shown in eq (9):

$$R_L = \frac{1}{1 + K_L C_0} \quad (9)$$

The R_L number indicates whether the adsorption affinity is irreversible ($R_L = 0$), favorable ($0 < R_L < 1$), linear ($R_L = 1$), or unfavorable ($R_L > 1$). In this study, the R_L value ranges [49] from 0.01 to 0.08 ($0 < R_L < 1$) and it corresponds to favorable adsorption of MB by kocho. The regression coefficient ($R^2 = 0.99845$) of the plot for Langmuir equation (8), which confirms that the adsorption process follows the Langmuir isotherm model, and the adsorption process mainly takes place via chemical interactions between the adsorbate and adsorbent. Thus, the outcomes suggested that the Langmuir model was the most appropriate one to explain the experimental data, which conveys the chemical interactions between the adsorbate and adsorbent [47]. The n value of kocho in the Freundlich model is 2.85. Since all of the n values are bigger than 1, this further supports the idea that the biosorption process will be effective at high MB concentrations.

Regeneration study

A desorption study helps to understand the reusability of the biosorbents, also reducing the cost of the biosorption process due to the reuse of the sorbents. In this study, 0.1 M HCl acid solutions at pH 2 are used as desorbents for kocho removal from MB-loaded biosorbent for five cycles. After each regeneration, a batch biosorption experiment was conducted to estimate the kocho regeneration ability using MB dye solution ($C_0 = 50 \text{ mg/L}$), contact time (50 min), pH (8) and 200 rpm agitation rate at 25 °C. As shown in Figure 8, the highest removal efficiency (94.2%) occurred during the first 50 min (Figure 8). The biosorption after the regeneration studies was very close to the initial efficiency, reducing only 3.8% from the initial dye removal after the fourth

cycle. More importantly, the biosorbent removal efficiency still shows 84.6% at the fifth cycle. As a result, the kocho biosorption ability is hardly affected after five cycle's uses, that is, only 9.6% decrease. Thus, it can be concluded that kocho is very applicable for removal of MB with good recycling ability.

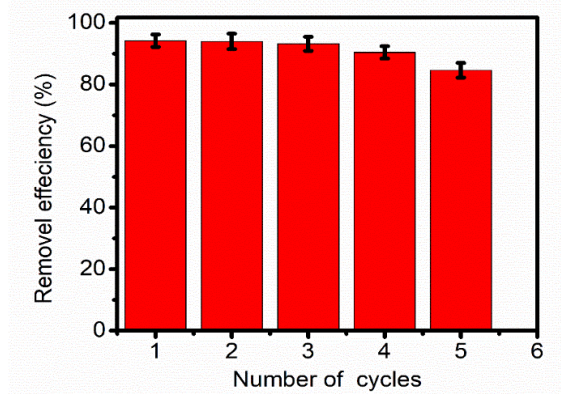


Figure 8. Reusability of adsorbent (kocho) for five cycle adsorption-desorption process.

Comparison of biosorption capacity of kocho with other biosorbents

A comparison of the candidate kocho's biosorption abilities for methylene blue as model cationic dye with those of different other adsorbents from literature was conducted. Compared to some of the biomaterials such as sawdust (89%) [20], banana fiber (85%) [20], eucalyptus sheathina bark and (86.33%) [22], the maximum MB removal efficiency was obtained by using kocho (94.2%). Thus, it can be concluded that the biosorbent kocho derived from pseudostem and corm of *Ensete ventricosum* (enset) is highly efficient for removal of MB dye from aqueous solution.

CONCLUSIONS

This study assesses potential of kocho derived from pseudostem and corm of *Ensete ventricosum* (enset) as a viable option for removing cationic MB dye from wastewater. Batch studies were performed to analyze the effects of dosage, initial MB concentration, pH and contact time. The results showed that the optimum parameters for biosorption process were 0.1 g of biosorbent dose, 50 mg/L MB concentration, pH 8 and contact time of 50 minutes. The highest removal efficiency was 94.2 % under the optimum experimental parameters. The experimental results indicate that the biosorption behavior of kocho followed pseudo-second order kinetic and Langmuir isotherm models. More importantly, kocho was very stable and can be easily recycled with 84.6% recovery after five cycles, which is convenient for the reusability of this material in wastewater treatments. In comparison with several adsorbents, the kocho is not only ecofriendly and economical but also the most efficient biomaterial to remove MB organic dye from aqueous system. Since kocho biosorbent has high porosity, cost effective, fast, easy availability, recycling ability, and abundant active sites on its surface, it should be considered as an excellent candidate for removal of dyes from wastewater. It implies that this research has a practical destination and is focused on the use of *Enset ventricosum* based biomaterial as a biosorbent in wastewater treatment.

ACKNOWLEDGMENTS

The authors would like to thank Debre Berhan University for providing laboratory facilities.

REFERENCES

1. Rathi, B.S.; Kumar, P.S.; Vo, D.N. Critical review on hazardous pollutants in water environment: Occurrence, monitoring, fate, removal technologies and risk assessment. *Sci. Total Environ.* **2021**, *797*, 149134.
2. Saravanan, A.; Senthil, K.P.; Jeevanantham, S.; Karishma, S.; Tajsabreen, B.; Yaashikaa, P.R.; Reshma, B. Effective water/wastewater treatment methodologies for toxic pollutants removal: Processes and applications towards sustainable development. *Chemosphere* **2021**, *280*, 130595.
3. Salleh, M.; Mahmoud, D.K.; Karim, W.; Idris, A. Cationic and anionic dye adsorption by agricultural solid wastes: A comprehensive review. *Desalination* **2011**, *280*, 1-13.
4. Badawi, A.K.; Abd Elkodous, M.; Ali, G.A. Recent advances in dye and metal ion removal using efficient adsorbents and novel nano-based materials: an overview. *Rsc. Adv.* **2021**, *11*, 36528-36553.
5. Djelloul, B.; Tabet, A.D.; Djillali, B. Adsorption of acid dye onto activated algerian clay. *Bull. Chem. Soc. Ethiop.* **2017**, *31*, 51-62.
6. Pavithra, K.G.; Jaikumar, V. Removal of colorants from wastewater: A review on sources and treatment strategies. *J. Ind. Eng. Chem.* **2019**, *75*, 1-19.
7. Yusuf, M. *Synthetic dyes: A threat to the environment and water ecosystem in Textiles and Clothing*, Wiley Online Library; **2019**, pp. 11-26.
8. Khan, I.; Saeed, K.; Zekker, I.; Zhang, B.; Hendi, A.H.; Ahmad, A.; Ahmad, S.; Zada, N.; Ahmad, H.; Shah, L.A. Review on methylene blue: Its properties, uses, toxicity and photodegradation. *Water* **2022**, *14*, 242.
9. Bayomie, O.S.; Kandeel, H.; Shoeib, T.; Yang, H.; Youssef, N.; El-Sayed, M. Novel approach for effective removal of methylene blue dye from water using fava bean peel waste. *Sci. Rep.* **2020**, *10*, 7824.
10. Mashkoor, F.; Nasar, A.; Asiri, A.M. Exploring the reusability of synthetically contaminated wastewater containing crystal violet dye using tectona grandis sawdust as a very low-cost adsorbent. *Sci. Rep.* **2018**, *8*, 1-16.
11. Solangi, N.H.; Kumar, J.; Mazari, S.A.; Ahmed, S.; Fatima, N.; Mubarak, N.M. Development of fruit waste derived bio-adsorbents for wastewater treatment: A review. *J. Hazard. Mater.* **2021**, *416*, 125848.
12. Ihsanullah, I.; Jamal, A.; Ilyas, M.; Zubair, M.; Khan, G.; Atieh, M.A. Bioremediation of dyes: Current status and prospects. *J. Water Process. Eng.* **2020**, *38*, 101680.
13. Nimesha, S.; Hewawasam, C.; Jayasanka, D.; Murakami, Y.; Araki, N.; Maharjan, N. Effectiveness of natural coagulants in water and wastewater treatment. *Glob. J. Environ. Sci. Manag.* **2022**, *8*, 101-116.
14. Mishra, S.; Cheng, L.; Maiti, A. The utilization of agro-biomass/byproducts for effective bio-removal of dyes from dyeing wastewater: A comprehensive review. *J. Environ. Chem. Eng.* **2021**, *9*, 104901.
15. Welde-Michael, G.; Bobosha, K.; Blomme, G.; Addis, T.; Mengesha, T.; Mekonnen, S. Evaluation of enset clones against enset bacterial wilt. *Afr. Crop. Sci. J.* **2008**, *16*, 89-95.
16. Tesfaye, B.; Lüdders, P. Diversity and distribution patterns of enset landraces in Sidama, Southern Ethiopia. *Genet. Resour. Crop Evol.* **2003**, *50*, 359-371.
17. Karssa, T.H.; Ali, K.A.; Gobena, E.N. The microbiology of Kocho: An Ethiopian traditionally fermented food from Enset (*Ensete ventricosum*). *Int. J. Life Sci.* **2014**, *8*, 7-13.

18. Karssa, T.; Papini, A. Effect of clonal variation on quality of Kocho, traditional fermented food from enset (*Ensete ventricosum*), Musaceae. *Int. J. Food Sci. Nutr. Eng.* **2018**, *8*, 79-85.
19. Nabieh, K.A.; Mortada, W.I.; Helmy, T.E.; Kenawy, I.; Abou El-Reash, Y.G. Chemically modified rice husk as an effective adsorbent for removal of palladium ions. *Heliyon* **2021**, *7*, 6062.
20. Rabia, R.; Iqra, M.; Liviu, M. Isothermal study of congo red dye biosorptive removal from water by solanum tuberosum and pisum sativum peels in economical way. *Bull. Chem. Soc. Ethiop.* **2018**, *32*, 213-223.
21. Mekuria, D.; Diro, A.; Melak, F.; Asere, T.G.; Rehman, R. Adsorptive Removal of Methylene Blue Dye Using Biowaste Materials: Barley Bran and Enset Midrib Leaf. *J. Chem.* **2022**, *2022*, 1-13.
22. Karthik, R.; Mutheshilan, R.; Jaffar, H.A.; Ramalingam, K.; Rekha, V. Effective removal of methylene blue dye from water using three different low-cost adsorbents. *Desalin. Water Treat.* **2016**, *57*, 10626-10631.
23. Afroze, S.; Sen, T.K.; Ang, M.; Nishioka, H. Adsorption of methylene blue dye from aqueous solution by novel biomass Eucalyptus sheathiana bark: equilibrium, kinetics, thermodynamics and mechanism. *Desalin. Water Treat.* **2016**, *57*, 5858-5878.
24. Jawad, A.H.; Hum, N.; Farhan, A.M.; Mastuli, M.S. Biosorption of methylene blue dye by rice (*Oryza sativa* L.) straw: adsorption and mechanism study. *Desalin. Water Treat.* **2020**, *190*, 322-330.
25. Zehra, T.; Priyantha, N.; Lim, L.B.; Iqbal, E. Sorption characteristics of peat of Brunei Darussalam V: removal of Congo red dye from aqueous solution by peat. *Desalin. Water Treat.* **2015**, *54*, 2592-2600.
26. Jiang, L.; Liu, Y.; Liu, S.; Hu, X.; Zeng, G.; Huang, B.; Li, M. Fabrication of β -cyclodextrin/poly (L-glutamic acid) supported magnetic graphene oxide and its adsorption behavior for 17β -estradiol. *J. Chem. Eng.* **2017**, *308*, 597-605.
27. Chang, Z.; Chen, Y.; Tang, S.; Yang, J.; Chen, Y.; Chen, S.; Li, P.; Yang, Z. Construction of chitosan/polyacrylate/graphene oxide composite physical hydrogel by semi-dissolution/acidification/sol-gel transition method and its simultaneous cationic and anionic dye adsorption properties. *Carbohydr. Polym.* **2020**, *229*, 115431.
28. D'Acerno, F.; Hamad, W.Y.; Michal, C.A.; MacLachlan, M.J. Thermal degradation of cellulose filaments and nanocrystals. *Biomacromolecules* **2020**, *21*, 3374-3386.
29. Shi, H.; Li, W.; Zhong, L.; Xu, C. Methylene blue adsorption from aqueous solution by magnetic cellulose/graphene oxide composite: equilibrium, kinetics, and thermodynamics. *Ind. Eng. Chem. Res.* **2014**, *53*, 1108-1118.
30. Ainane, T.; Khammour, F.; Talbi, M.; Elkouali, M.H. A novel bio-adsorbent of mint waste for dyes remediation in aqueous environments: study and modeling of isotherms for removal of methylene Blue. *Orient. J. Chem.* **2014**, *30*, 1183-1189.
31. Sofla, MR.K.; Brown, R.; Tsuzuki, T.; Rainey, T. A comparison of cellulose nanocrystals and cellulose nanofibres extracted from bagasse using acid and ball milling methods. *Adv. Nat. Sci. J. Nanosci.* **2016**, *7*, 035004.
32. Han, R.; Zou, W.; Yu, W.; Cheng, S.; Wang, Y.; Shi, J. Biosorption of methylene blue from aqueous solution by fallen phoenix tree's leaves. *J. Hazard. Mater.* **2007**, *141*, 156-162.
33. Khodabandehloo, A.; Rahbar-Kelishami, A.; Shayesteh, H. Methylene blue removal using *Salix babylonica* (Weeping willow) leaves powder as a low-cost biosorbent in batch mode: Kinetic, equilibrium, and thermodynamic studies. *J. Mol. Liq.* **2017**, *244*, 540-548.
34. Ahmad, A.; Mohd-Setapar, S.H.; Chuong, C.S.; Khattoon, A.; Wani, W.A.; Kumar, R.; Rafatullah, M. Recent advances in new generation dye removal technologies: novel search for approaches to reprocess wastewater. *Rsc. Adv.* **2015**, *5*, 30801-30818.

35. Kaur, S.; Jindal, R.; Kaur, B. J. Synthesis and RSM-CCD optimization of microwave-induced green interpenetrating network hydrogel adsorbent based on gum copal for selective removal of malachite green from waste water. *Polym. Eng. Sci.* **2018**, *58*, 2293-2303.
36. Sen, T.K.; Afroze, S.; Ang, H. Equilibrium, kinetics and mechanism of removal of methylene blue from aqueous solution by adsorption onto pine cone biomass of *Pinus radiata*. *Water Air Soil Pollut.* **2011**, *218*, 499-515.
37. Abd El-Latif, M.; Ibrahim, A.M.; El-Kady, M. Adsorption equilibrium, kinetics and thermodynamics of methylene blue from aqueous solutions using biopolymer oak sawdust composite. *Am. J. Sci.* **2010**, *6*, 267-283.
38. Rahman, M.A.; Amin, S.R.; Alam, A.S. Removal of methylene blue from waste water using activated carbon prepared from rice husk. *Dhaka Univ. J. Sci.* **2012**, *60*, 185-189.
39. Liu, Y.; Huang, S.; Zhao, X.; Zhang, Y. Fabrication of three-dimensional porous β -cyclodextrin/chitosan functionalized graphene oxide hydrogel for methylene blue removal from aqueous solution. *Colloids Surf. A: Physicochem. Eng. Asp.* **2018**, *539*, 1-10.
40. Ngah, W.W.; Hanafiah, M.M. Removal of heavy metal ions from wastewater by chemically modified plant wastes as adsorbents: a review. *Bioresour. Technol.* **2008**, *99*, 3935-3948.
41. Shakoor, S.; Nasar, A. Removal of methylene blue dye from artificially contaminated water using citrus limetta peel waste as a very low cost adsorbent. *J. Taiwan. Inst. Chem. Eng.* **2016**, *66*, 154-163.
42. Mosoarca, G.; Vancea, C.; Popa, S.; Dan, M.; Boran, S. The use of bilberry leaves (*Vaccinium myrtillus* L.) as an efficient adsorbent for cationic dye removal from aqueous solutions. *Polym.* **2022**, *14*, 978.
43. Mosoarca, G.; Vancea, C.; Popa, S.; Gheju, M.; Boran, S. Syringa vulgaris leaves powder a novel low-cost adsorbent for methylene blue removal: Isotherms, kinetics, thermodynamic and optimization by Taguchi method. *Sci. Rep.* **2020**, *10*, 1-9.
44. Boumaza, S.; Yenounne, A.; Hachi, W.; Kaouah, F.; Bouhamidi, Y.; Trari, M. Application of *Typha angustifolia* (L.) dead leaves waste as biomaterial for the removal of cationic dye from aqueous solution. *Int. J. Environ. Res.* **2018**, *12*, 561-573.
45. Ho, Y.; McKay, G. A comparison of chemisorption kinetic models applied to pollutant removal on various sorbents. *Trans I Chem E* **1998**, *76*, 332-340.
46. Ho, Y.S.; McKay, G. Pseudo-second order model for sorption processes. *Process. Biochem.* **1999**, *34*, 451-465.
47. Jawad, A.H.; Hum, N.; Farhan, A.M.; Mastuli, M.S. Biosorption of methylene blue dye by rice (*Oryza sativa* L.) straw: Adsorption and mechanism study. *Desalin. Water. Treat.* **2020**, *190*, 322-330.
48. Freundlich, H. Über die adsorption in lösungen. *Z. Phys. Chem.* **1907**, *57*, 385-470.
49. Hall, K.R.; Eagleton, L.C.; Acrivos, A.; Vermeulen, T. Pore-and solid-diffusion kinetics in fixed-bed adsorption under constant-pattern conditions. *Ind. Eng. Chem. Fundamen.* **1966**, *5*, 212-223.